

www.wcee2024.it

MULTI-OBJECTIVE OPTIMIZATION OF CROSS-LAMINATED TIMBER SHEAR WALLS

G. B. Shargh¹, A. Barbosa², B. Simpson³, A. Sinha⁴, J.W. van de Lindt⁵ & N.C. Brown⁶

- ¹ Department of Architectural Engineering, Pennsylvania State University, State College, USA, Boshrouei@psu.edu
 - ² School of Civil & Construction Engineering, Oregon State University, Corvallis, USA
 - ³ Department of Civil and Environmental Engineering, Stanford University, Stanford, USA
 - ⁴ Department of Wood Science & Engineering, Oregon State University, Corvallis, USA
- ⁵ Department of Civil and Environmental Engineering, Colorado State University, Fort Collins, USA
 - ⁶ Department of Architectural Engineering, Pennsylvania State University, State College, USA

Abstract: According to a new design paradigm called Converging Design, high-level optimization objectives such as resilience and sustainability can be pursued through iterative simulation and feedback. Unlike traditional design processes that prioritize desirable seismic performance at various seismic hazard levels, the Converging Design methodology also considers the long-term ecological impact of construction and functional recovery. This methodology requires navigating competing priorities, which can be pursued through multiobjective optimization (MOO). However, computational costs and incorporating uncertainty in seismic analysis also demand that optimization frameworks use algorithms and analysis resolutions that are appropriate to the decisions being made as the design is refined. While such a framework could be applied to any material, mass timber systems are increasingly attractive as a potential sustainable solution for buildings. In this study, using a Python-based object-oriented program, an automated structural design procedure is developed to evaluate the seismic and sustainability performance of parametrically definable mass timber building configurations. Different geometric classes with Cross-Laminated Timber Rocking Walls are modeled using OpenSees and are automatically designed. Their behavior is then studied to provide insights into the relationship between structural variables and the optimization objectives. The results show a clear trade-off between Seismic Safety (the inverse of risk) and Global Warming Potential due to the construction of different design options, although the nature of this trade-off depends on the desired seismic behavior limit states. The developed software thus enables designers to efficiently explore a range of early design options for mass timber lateral systems and to achieve optimal solutions that balance seismic and sustainability performance.

1 Introduction

Mass timber building systems have become increasingly prevalent in recent years, largely due to sustainability concerns (Sandoli, 2021). Mass timber structural systems can display robust seismic behavior that is competitive with their steel and concrete counterparts. However, many lateral systems in tall timber buildings still contain significant amounts of steel or concrete, which can have outsized effects on the overall embodied carbon or other environmental impacts of the building construction. Ongoing research has sought to incorporate more mass timber and less of these other materials in new seismic force-resisting systems, although at minimum many connections and other small components are still made from steel to dissipate energy. Such hybrid timber-steel systems enable efficient allocation of energy-dissipating elements, primarily constructed from ductile materials (e.g., steel), while simultaneously lowering the carbon footprint by

incorporating mass timber as the dominant material. Hence, distinct seismic performance objectives can be achieved by careful design of the ductile components with respect to the desired performance.

In the case of a Cross Laminated Timber (CLT) mass timber rocking wall system, recentering and energy dissipating behaviors are provided by post-tensioned (PT) bars and special devices such as U-shaped flexural plates (UFPs), respectively, while the CLT panel mostly resists lateral forces through its weight in low levels of intensity, and its crushing at the toe at high levels of seismic demand. Experimental and numerical evaluations of CLT structures have displayed their ability to perform to desired levels during earthquakes (van de Lindt, 2019; Wichman, 2022; Lukacs, 2019; Ganey, 2015; Massari, 2017). At the same time, comparative assessments show that CLT buildings have significant potential to reduce energy consumption and CO₂ emissions compared with other materials (Younis and Dodoo, 2022; Liu, 2016; Guo, 2017; Piacenza, 2013; Kontra, 2023).

Like many engineering problems, the desired objectives of enhanced seismic performance and reduced carbon footprint can result in trade-offs. In most cases, there exists a dispensable trade-off between the amount of material used in the Lateral Force-Resisting System (LFRS) of a structure and its vulnerability. There have been several studies taking the concurrent impact of seismic and climate considerations of other types of LFRS systems into account (Manfredi and Masi, 2018; Menna, 2019). This paper contributes to existing knowledge by considering relationships between these objectives in the case of the CLT rocking wall system, which has not been thoroughly studied before. Given the range of design variables in rocking wall systems that affect both goals, multi-objective optimization techniques can help analyze possible scenarios and provide designers with information about the nature of the trade-offs. Optimization has been applied to seismic design problems as discussed in Zakian and Kaveh (2023) and Lagaros (2008); however, in this study, seismic objectives are viewed as optimization constraints, as discussed later.

Previous applications of multi-objective optimization to this problem have been limited due to the high computational costs of simulating seismic response in buildings and the relatively unknown performance of mass timber lateral systems prior to recent full-scale tests. In response, we employ a multi-objective approach to generate and analyze CLT rocking wall system designs for two classes of 2-story and 5-story buildings. In each class, the seismic risk is calculated based on different assumptions for the Maximum Inter-story Drift Ratios, showing the resulting non-dominated design solutions along with the global warming potential of each system. The simulations rely on sampling a Python-based parametric structural model that incorporates variables controlling the number, location, and size of various components, along with the post-tensioning force applied. OpenSeesPy (Zhu, 2018) is used within the algorithm to evaluate 115 different 2-dimensional CLT buildings. The variable space of these simulations is also analyzed, showing which settings control both performance objectives in the different scenarios. Having designs with both seismic and sustainability qualities and demonstrating the comparable competencies of mass timber structures can add to their appeal as an efficient solution for construction in seismic regions, while at the same time addressing broader environmental concerns.

2 Methodology

2.1. Building case studies and optimization formulation

The first step of the optimization process is to select the building context and location. In this study, Los Angeles is chosen as the construction site, and the studied buildings have regular office loading. Next, a *Geometric Class* that includes the lengths of spans and the heights and number of stories is chosen. In the current study, two parametric 2-story and 5-story buildings are set as geometric classes to represent low-rise and mid-rise mass timber structures. The analysis model assumes a two-dimensional (2D) system, shown in Figure 1 along with different structural components and their locations. In all models, the heights are 3.66 m and 3.05 m for the first and rest of the stories, respectively. The gravity frame spans are 2.28 m. The optimization problem is defined as:

$$\min_{x \in \Omega} (\lambda, \gamma)$$
 Subject to $g_k(x) \le 0 \quad k=1, 2 ..., p$ (1)

where, λ is the annual rate of exceeding a Limit State of Maximum Inter-story Drift Ratio (LS_{MIDR}), generally called seismic risk, γ is the global warming potential of the lateral system, Ω is the design variables domain, x is a sample vector of design variables, $g_k(x)$ is the generic constraint expression that is satisfied when negative, and p is the number of constraints. The following sections detail the parameters, variables, objectives, and constraints, before discussing the algorithm used to produce the design options.

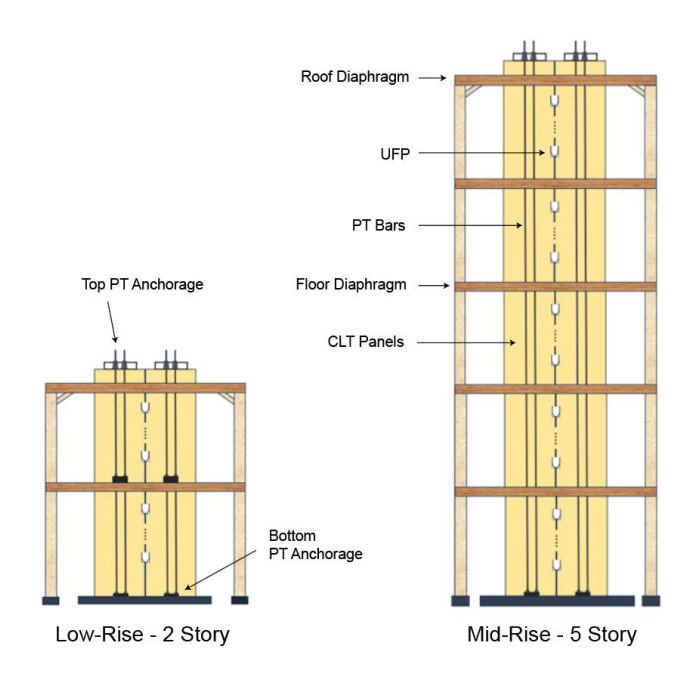


Figure 1. Schematic figures of building classes.

2.2. Parameters and variables

The adjustable simulation properties include Design Variables (DV), Design Parameters (DP), and Modeling Parameters (MP), shown in Figure 2. Following typical conventions in multi-disciplinary design optimization (Agte, 2010), *Design Variables* directly contribute to the evaluation of the objectives and are adjusted during the optimization process. An example is the dimension of the UFPs, which can be specified by the designer to influence the performance. Eight design variables are incorporated, involving timber panels, steel rods, and steel UFPs. *Design Parameters* encompass general characteristics of an optimization run, which in turn lead to different design spaces that can implicitly impact the optimal values of objectives and optimization space. For instance, site location or the number of stories determine the specific seismic design loads, by which the entire design space and optimal designs are shaped. *Modeling Parameters* pertain to the assumptions made in the OpenSees code. An example is the number of springs under the walls that model the rocking behavior. This parametric flexibility provides a robust framework for evaluating the performance of a broad spectrum of mass timber rocking wall lateral systems in alignment with the user's specific requirements.

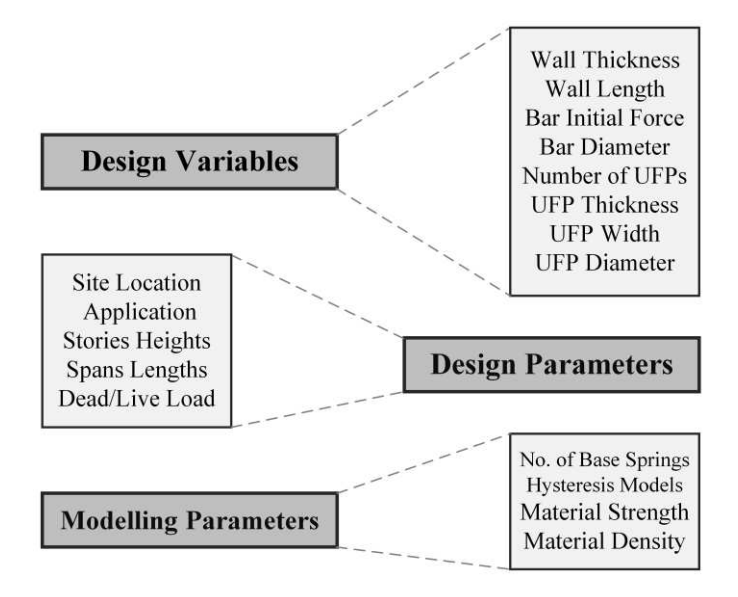


Figure 2. Design Variables, Design Parameters, and Modeling Parameters along with their members.

Table 1 presents the upper and lower bounds of each Design Variable and their units. *Wall Thickness* depends on the number of plies employed in manufacturing the CLT panels, which are taken as an integer between 3 and 9 based on what would typically be available in practice (SmartLam, 2020). *Bar Initial to Yield Force Ratio* is the initial post-tension (PT) force in the bars relative to the yield force of the element. *Story No. of UFPs* is the total count of U-shaped flexural plates (UFP) elements that are used in each story. The *Bar Diameter* and *UFP Thickness* are defined as integer values according to common sizes (Baird, 2014). The result is a mix of continuous and discrete variables, which can influence the available optimization algorithms. In this paper, a decision was made to use sampling and post-Pareto analysis rather than an automated MOO algorithm, largely due to the relative computational costs for different problem components and the fact that this process is conceived as part of a larger approach to providing feedback at varying stages of building design. These influences are described in later sections.

Table 1: Design Variables, their units, and range of variation.

Design Variable	Lower Bound	Upper Bound	Variable Type
Wall Thickness (m)	0.1	0.3	Discrete
Wall Length (m)	1	3	Continuous
Bar Diameter (mm)	16	50	Discrete
Bar Initial to Yield Force Ratio	0.1	0.9	Continuous
Story No. of UFPs	2	7	Discrete
UFP Width (mm)	80	110	Continuous
UFP Thickness (mm)	5	12	Discrete
UFP Diameter (mm)	60	140	Continuous

2.3. Constraints

In performance-based design, structures are designed to exhibit distinct suitability at different hazard levels. Predetermined hazard levels thus define seismic performance objectives associated with that level. For each design sample considered in this study, nine seismic constraints are evaluated to determine its eligibility. A design is dismissed unless it satisfies the seismic performance objectives (PO) considered. In this respect, each PO can be regarded as a constraint of the optimization process. The seismic performance objectives are as proposed by (Busch, 2022), while seismic demands are computed by the ELF (Equivalent Lateral Force) method per ASCE 7 2022. To facilitate the evaluation process, an approximation method is employed, which is based on the cross-section analysis procedure and the monolithic beam analogy. This simplifying procedure was first proposed for precast concrete frames (Pampanin, 2001), and then utilized by (Newcombe, 2008; Ganey, 2015; Wichman, 2022) for mass timber structures.

In the context of optimization, the *objective* is a reserved terminology that represents the quantity that is meant to be optimized. The seismic performance objectives will thus be referred to as *constraints* in the rest of this study. The constraints for this problem are:

- 1. Building drift should be limited to 2% under the DE (Design Earthquake).
- 2. Building drift should be limited to 4% under the MCE_R (Risk-Targeted Maximum Considered Earthquake).
- 3. The restoring ratio of the rocking wall should be greater than 1.
- 4. The wood crushing at the wall toe should be limited under the DE.
- 5. To recenter the wall, PT elements must not yield under the DE.
- 6. PT elements are not permitted to rupture under the MCE_R.
- 7. Energy-dissipation elements (UFPs) should not fail under the MCE_R.
- 8. The UFP energy dissipation ratio should be greater than 0.25.
- 9. Moment and shear capacity checked against the LRFD (Load and Resistance Factor Design) moment and shear demand using ELF.

2.4. Objectives

Seismic Risk

The first optimization objective to be minimized is the seismic risk. The risk assessment captures various uncertainties in the earthquake occurrence and structural response, to estimate the potential adverse outcomes resulting from earthquakes on the structures. It is expressed in terms of the probabilities of potential adverse impact on buildings and infrastructure within a specified period. Seismic risk is influenced by a range of factors but is generally a function of the level of seismicity of the region and the vulnerability of the structure. In this study, the Maximum Inter-story Drift Ratio (MIDR) is regarded as the Engineering Demand Parameter (EDP), and the probability of exceeding three MIDR limit states of 0.01, 0.02, and 0.04 are calculated. The pseudo-acceleration at the first mode of vibration is regarded as the ground motion Intensity Measure (IM), based on which the Probabilistic Seismic Hazard Analysis (PSHA) is conducted for the site location. Eventually, given each limit state LS_{MIDR} , the annual rate of exceedance is computed using Eq. 2.

$$\lambda(\text{MIDR} > \text{LS}_{\text{MIDR}}) = \int_0^\infty P(\text{MIDR} > \text{LS}_{\text{MIDR}} | \text{Sa}(\text{T}_1) = \text{Sa}) \left| \frac{d\lambda(\text{Sa}(\text{T}_1) > \text{Sa})}{d\text{Sa}} \right| d\text{Sa}$$
 (2)

where $\lambda(Sa(T_1) > x)$ is the ground-motion hazard curve derived from PSHA and $P(MIDR > LS_{MIDR} | Sa(T_1) = Sa)$ is the fragility function of exceeding the limit state LS_{MIDR} . There are multiple methods to derive this function (Baker, 2015). In this study, fragility functions are calculated utilizing Cloud Analysis (Cornell, 2002) through Eq. 3.

$$P(MIDR>LS_{MIDR}|S_a)=1-P(MIDR(3)$$

$$\ln \eta_{\text{MIDR}|S_a} = \ln a + b \ln \text{Sa}(T_1)$$
 (4)

$$\beta_{\text{MIDR}|S_a} = \sqrt{\frac{\sum_{i=1}^{N} (\ln(\text{MIDR}_i) - \ln\eta_{\text{MIDR}|S_{a,i}})^2}{N-2}}$$
 (5)

Where, $P(MIDR > LS_{MIDR} | Sa)$ is the probability of exceeding LS_{MIDR} at the level of Sa, $\eta_{MIDR | Sa}$ is the median of MIDR limit state at Sa, estimated using linear regression with the coefficients of a and b, $\beta_{MIDR | Sa}$ is the residual standard error of the regression, and $\Phi(.)$ is the standardized Gaussian distribution function. As proposed by (Shargh and Barati, 2023), in the context of Cloud Analysis, there exists an *Optimal Rotational Angle* for a pair of structure-ground motion, through which the resulting fragility function can encompass more comprehensive information about the behavior of the structure compared with the as-recorded angles. In other words, employing these optimal angles can significantly reduce the computational costs while preserving the precision required for structural behavior estimation. This approach proves particularly advantageous in seismic performance assessment problems that call for substantial computational resources such as optimization. Table 2 presents the original ground motions utilized in this process along with their characteristics.

Global Warming Potential

Due to the increased emphasis on the upfront environmental impact of buildings, Global Warming Potential (GWP) is the second objective for minimization. This metric is a broad measure of sustainability using a mass of CO₂ equivalent (kg-CO₂e) as the primary unit. In the component manufacturing process, various greenhouse substances like nitrous oxide, methane, and ozone are emitted, whose adverse impacts may surpass that of CO₂ (Lashof and Ahuja, 1990). However, an equivalent measure known as CO₂e is proposed to account for all, reflecting the general level of greenhouse gas emissions. The GWP is computed by Equation 6.

$$Y = \sum_{k=1}^{n} C_k^* \alpha_k \tag{6}$$

Where, the amount of each material, in terms of the required base unit, α_k , is multiplied by the corresponding GWP coefficient, C_k , yielding the total GWP of the design. The values of C_k coefficients are as prescribed by Waldman (2023) and as presented in Table 3. These baseline coefficients assume cradle-to-gate contributions

to Global Warming Potential, or A1-A3 of the product stage in a typical life cycle assessment (LCA). Although coefficients for additional stages could be assumed instead, this would require more specificity than is available for the selected case studies at this time.

Table 2: Characteristics of selected ground motions.

Record Sequence Number	Earthquake Name	Magnitude	Mechanism	Rjb (km)	Vs30 (m/sec)	Soil Type	PGA (g)
15	Kern County	7.36	Reverse	38.42	385.43	С	0.07
68	San Fernando	6.61	Reverse	22.77	316.46	D	0.10
183	Imperial Valley	6.53	Strike slip	3.86	206.08	D	0.23
236	Mammoth Lakes	5.91	Strike slip	2.67	382.12	С	0.11
442	Borah Peak	5.1	Normal	16.31	468.44	С	0.02
1549	Chi-Chi	7.62	Reverse Oblique	1.83	511.18	С	0.77
4895	Chuetsu-Oki	6.8	Reverse	0	265.5	D	0.40
5482	lwate	6.9	Reverse	13.07	458.73	С	1.49
5657	lwate	6.9	Reverse	0	506.44	С	0.76
8157	Christchurch	6.2	Reverse Oblique	0	422	С	0.64

Table 3: Employed Carbon Leadership Forum Coefficients.

Material	Rebar - fabricated	Plate steel-fabricated	CLT
CLF Baseline GWP (kg CO₂e)	854/ton	1730/ton	137.19/m ³

2.5. Optimization algorithm

An overview of the optimization process is provided in Figure 3. As described at the beginning of this section, the process begins by choosing a location and creating a geometric class. Although many typical MOO procedures employ an automated algorithm to progressively push towards a more efficient Pareto set, this process uses sampling and filtering instead. This is because of the relative computational demands of the design checks versus the full computation of the first objective function, which are detailed in Figure 4. As presented, 10,000 samples are initially generated for each *Geometric Class* out of which 53 and 62 samples could satisfy the seismic constraints for 2- and 5-story classes, respectively. While the design checking process for all 10,000 samples only takes 17 minutes on a typical professional workstation, with the same computational power, seismic assessment of 2- and 5-story classes respectively require 38.8 and 106.3 hours of computation on average. Given that the checks are much more efficient, it was decided to conduct the sampling first, rather than have them incorporated into an automated constrained MOO algorithm, which was shown to be the most efficient process for similar problems (Zargar, 2023).

3 Results

For each geometric class, 10,000 samples are generated using the Latin Hypercube Method (Iman, 1981). By conducting the described algorithm, 53 and 62 realizations (i.e., building structures) are respectively qualified for the 2- and 5-story geometric classes. Then, for each of the 115 buildings, the Cloud Analysis is conducted and associated objective values are calculated. Regarding the idiosyncratic fundamental period of each building and the employment of ten original ground motions, 1150 different waveforms and Nonlinear Time-History Analyses are utilized and conducted. As shown before, the original records selected to have a wide range of ground shaking intensity, and each one is rotated to the optimal angle proper for the structure-ground motion. Figure 5 presents the objective values for the whole sample sets for both geometric classes, indicating dominated samples in grey and Pareto front designs in a gradient color palette from blue, as the highest risk, to red, as the lowest risk value.

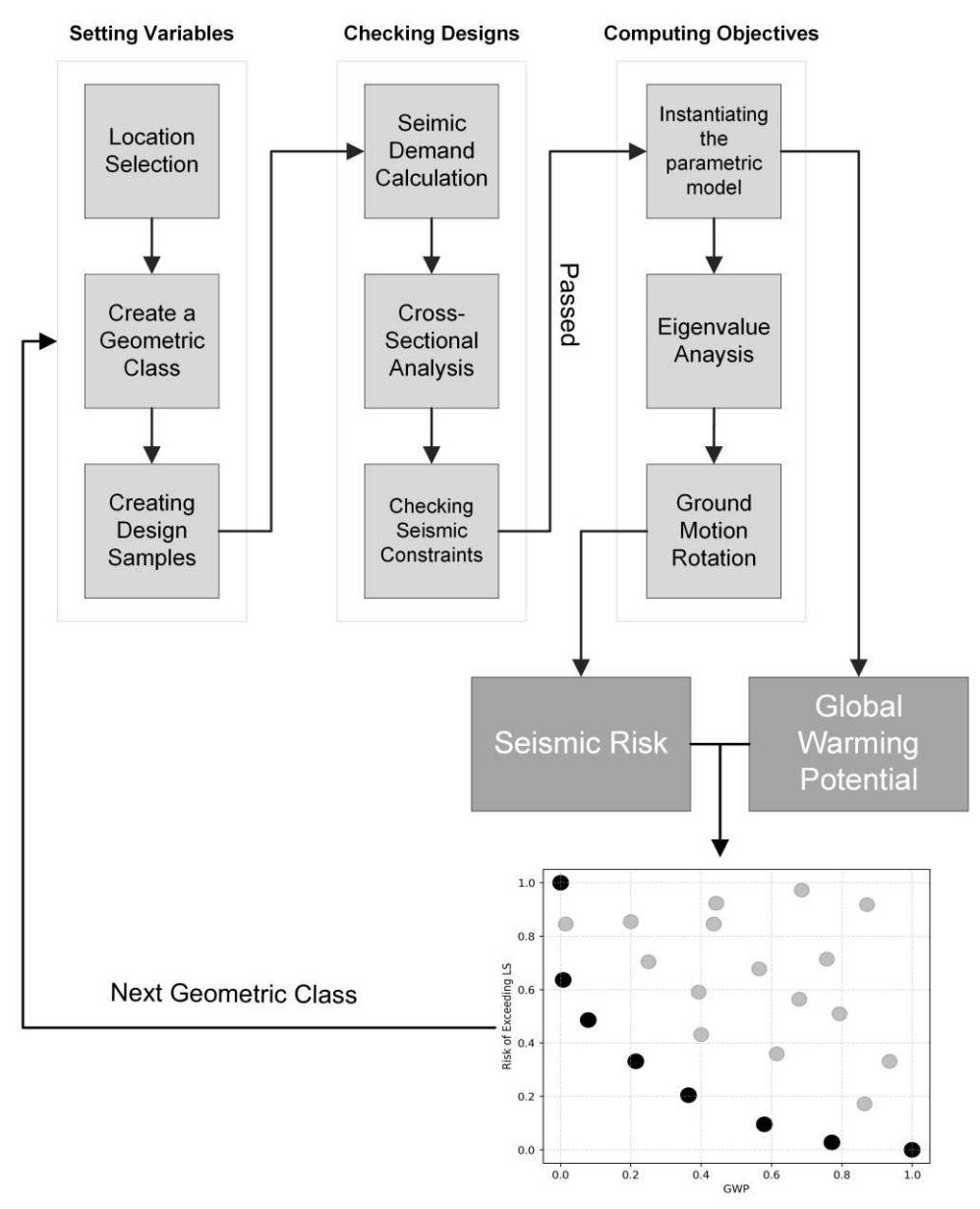


Figure 3. The flowchart of the design exploration.

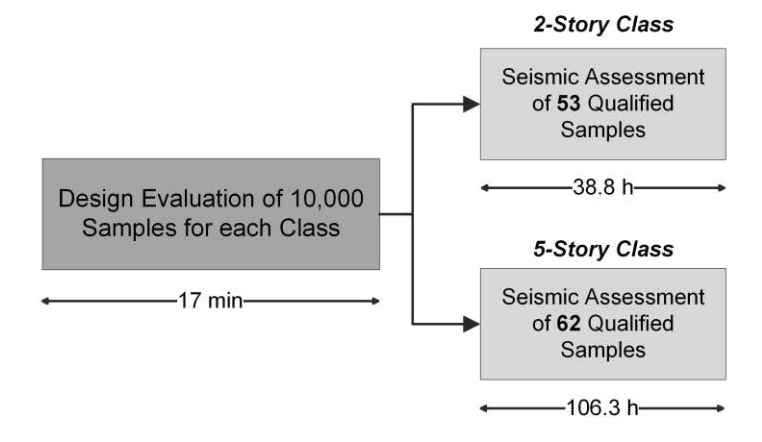


Figure 4. Comparison of the computational cost of constraints and seismic assessment evaluation.

The color gradient can provide insights into not only the relationship between the objectives but also the roles of Design Variables in determining the objective values. As a preliminary inspection, plots demonstrate sparser point densities as the seismic risk increases for all cases. This observation is directly attributed to the fact that the seismic constraints have filtered a wide range of designs with elevated levels of seismic risk.

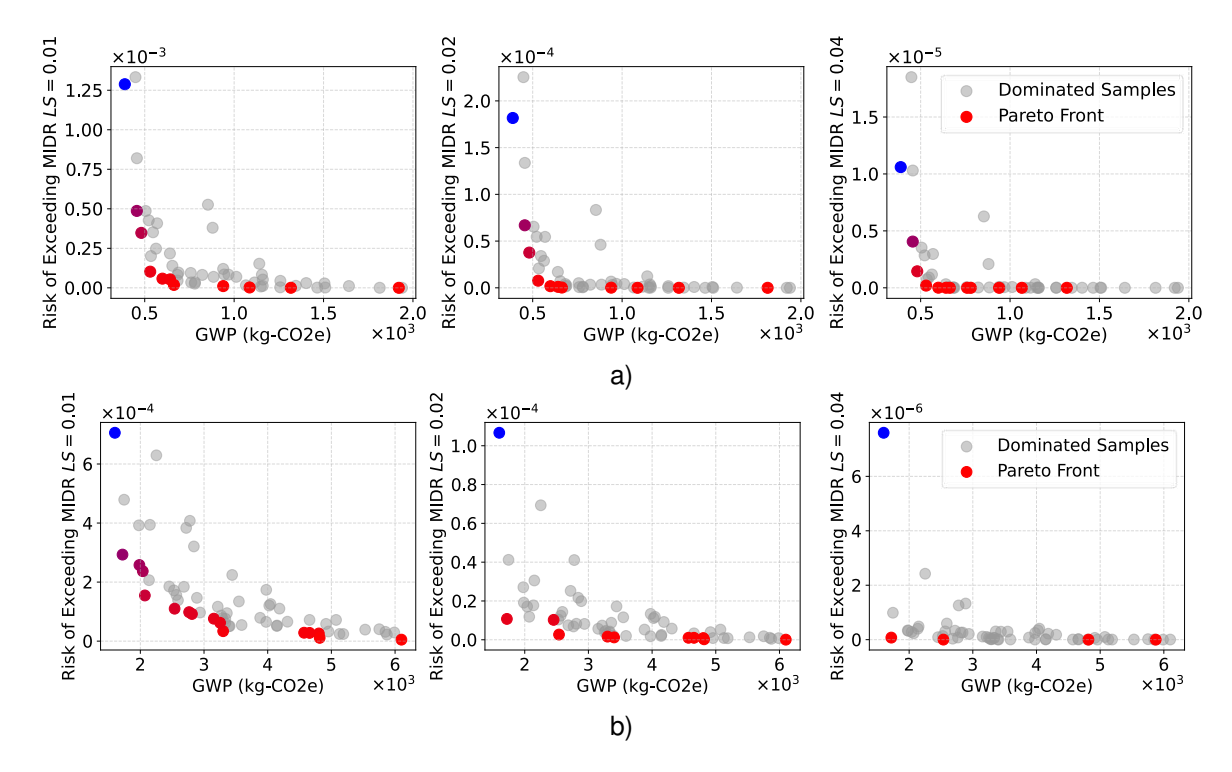


Figure 5: The entire sample sets and Pareto cases for two classes: a) LS_{MIDR}=0.01, 0.02, and 0.04 of 2-story class b) LS_{MIDR}=0.01, 0.02, and 0.04 of 5-story class.

As can be seen, there exists a natural trade-off between the two considered objectives. However, the Pareto fronts have specific trends that are functions of the limit state level and geometric class. Pareto optimal designs of 2-story buildings show an almost constant level of seismic risk for a wide range of GWP values for all limit states. For example, in the case of LS_{MIDR}=0.01 for the 2-story class, the Pareto cases with GWP greater than 650 kg-CO₂e lead to almost equal and small quantities of seismic risk. This observation remains valid for higher limit states with approximately the same level of GWP. It implies that providing high levels of safety is possible across a wide range of GWP values. However, as expected, the level of exceedance probability reduces for limit states corresponding to higher nonlinearity. On the other hand, in the 5-story geometric class, the seismic risk quantities are more sensitive to the sustainability metric. For instance, at LS_{MIDR}=0.01, the risk of exceedance monotonically decreases as more amounts of GWP engage in the design. It indicates a stronger need for carbon consumption to reduce the level of risk. This trend is more pronounced in mid-rise structures when compared with low-rise ones across all limit states.

Figure 6 illustrates the seismic risk against all Design Variables for the 2-story class over different limit states. As shown, the strong inverse correlation between the risk and Wall Length is apparent, which is highlighted due to the concentration of low-risk Pareto cases at high Wall Lengths. Also, a Wall Length equal to 1m on the Pareto front led to the lowest level of safety, with near-average values over most of the other Design Variables. These observations speak for the importance of this DV in the seismic risk. Moreover, the safer buildings among Pareto cases have large values of UFP Thickness and Width. This observation holds true for all limit states. In contrast, Pareto cases are denser over the range of samples with the smallest UFP diameters. This is due to the inverse relationship from the UFP diameter to the UFP yield force and stiffness (Baird, 2014), since incrementing the UFP diameter increases GWP. Furthermore, safer buildings are inclined to have high bar force ratios, which is representative of the initial post-tensioning force, and the greater number of UFPs, albeit with lesser significance compared to Wall Length. Given this dataset, no discernible relationship exists between the Number of Plies and Bar Diameter and the risk value, as the Pareto cases are evenly distributed across their respective ranges of consideration. The mentioned observations are almost identical at all limit

states. Figure 7 illustrates the Risk of exceedance with respect to each DV for the 5-story class buildings for three LSs. It is interesting to note that similar observations to that of the 2-story class can be made again for all limit states. The decisive impact of Wall Length and UFP thickness, which is directly related to the stiffness and yield force of UFP with a power of 2 and 3, respectively, are evident through the distribution of Pareto cases.

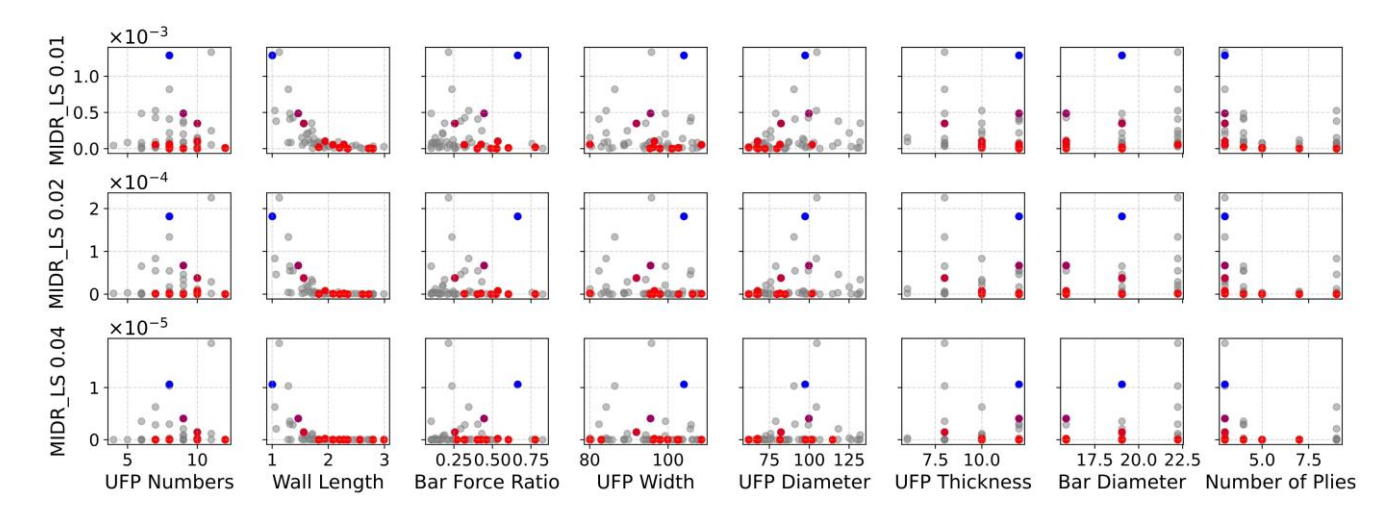


Figure 6: Risk of different limit states against Design Variables for 2-story class.

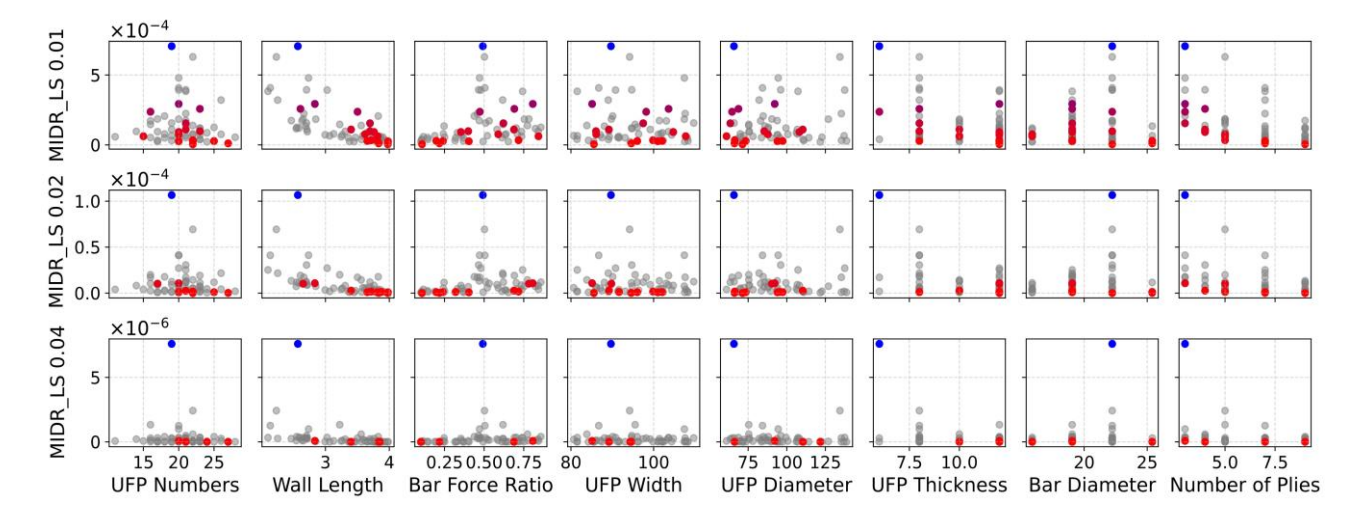


Figure 7: Risk of different limit states against Design Variables for 5-story class.

Figures 8 and 9 depict the GWP objective values versus each Design Variable respectively for 2-story and 5-story classes. It should be noted that the Pareto cases are based on the GWP-Risk plot corresponding to LS_{MIDR}=0.01. The figures show that GWP is directly linked to the Wall Length and the Number of Plies, more than any other Design Variable. Entire sample sets and Pareto samples are dispersed over the range of other Design Variables with lower correlations. However, the Bar Force Ratio variable has a more meaningful relationship with GWP in the case of the taller class of structures.

4 Discussion and Conclusions

This research demonstrates a Converging Design approach for timber structural systems, specifically Cross-Laminated Timber Rocking Shear Walls. Using a Python-based object-oriented program and OpenSeesPy, an automated structural design procedure was developed to model, design, and evaluate two general 2- and 5-story CLT structure classes in terms of seismic and sustainability performance with parametrically definable building configurations.

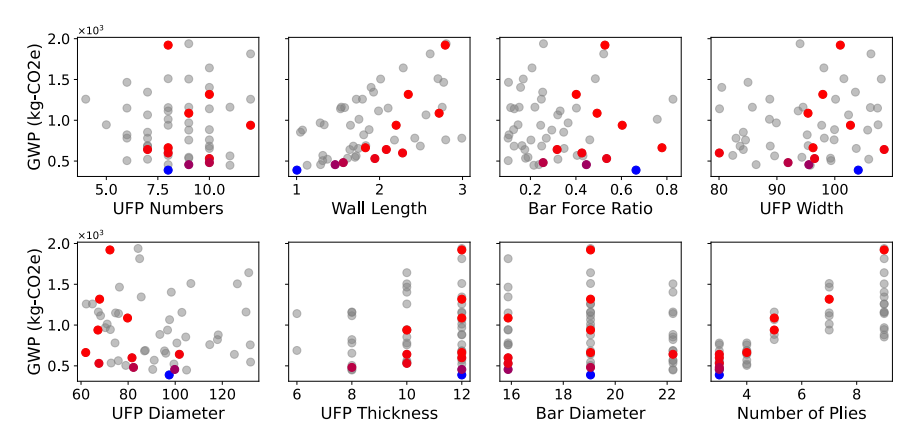


Figure 8: GWP against Design Variables for 2-story-class buildings including (Pareto samples associated with $LS_{MIDR}=0.01$).

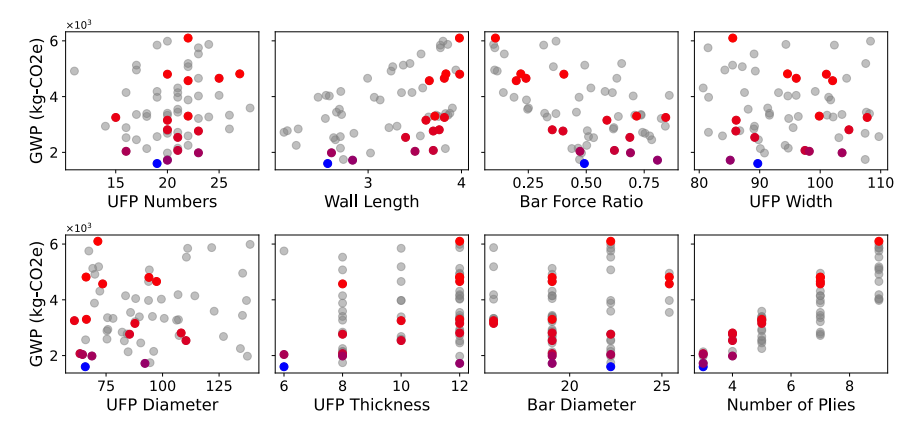


Figure 9: GWP against Design Variables for 5-story-class buildings including (Pareto samples associated with LS_{MIDR}=0.01).

The results of this study shed light on the trade-off between the seismic risk of exceeding 0.01, 0.02, and 0.04 maximum inter-story drift ratio limit states and global warming potential. Pareto fronts are shown to be dependent on the limit state level and geometric class. Notably, 2-story buildings show a relatively constant level of seismic risk across a wide range of GWP values, indicating that high levels of safety can be achieved without exceeding a certain sustainability threshold. On the other hand, mid-rise structures (5-story buildings) are more sensitive to sustainability measures, highlighting the higher need for carbon consumption to lower the seismic risk. Furthermore, the analysis of design variables revealed key insights into their impact on seismic risk and GWP. Wall Length, UFP Thickness, and Width are demonstrated to be crucial factors influencing seismic risk, while GWP is most strongly linked to Wall Length and the Number of Plies. The observations regarding these variables were consistent across different limit states and geometric classes. Future advancements such as leveraging machine learning methods have the potential to significantly reduce the computational expenses associated with these problems. In addition, there is room for a more exhaustive exploration of GWP in the context of overall building lifecycles. Both areas of future work could contribute to further exploration of the interplay between seismic performance and sustainability for mass timber buildings.

5 Acknowledgments

This research was funded by the National Science Foundation (NSF) under awards #2120683, #2120692, and #2120684. We also recognize the USDA Agricultural Research Service, the TallWood Design Institute, and their industry partners for their contributions to the experimental program. Any opinions, findings, and conclusions are those of the authors and do not necessarily reflect the views of the supporting agencies.

6 References

Agte, J., De Weck, O., Sobieszczanski-Sobieski, J., Arendsen, P., Morris, A. and Spieck, M. (2010). MDO: assessment and direction for advancement—an opinion of one international group. *Structural and Multidisciplinary Optimization*. *40*, pp.17-33.

- Baird, A., Smith, T., Palermo, A. and Pampanin, S. (2014). Experimental and numerical study of U-shape flexural plate (UFP) dissipators. New Zealand Society for Earthquake Engineering 2014 Technical Conference and AGM.
- Baker, J.W., 2015. Efficient analytical fragility function fitting using dynamic structural analysis. Earthquake Spectra, 31(1), pp.579-599.
- Busch, A., Zimmerman, R.B., Pei, S., McDonnell, E., Line, P. and Huang, D. (2022). Prescriptive seismic design procedure for post-tensioned mass timber rocking walls. *Journal of Structural Engineering*, *148*(3), p.04021289.
- Ceccotti, A. (2008). New technologies for construction of medium-rise buildings in seismic regions: the XLAM case. *Structural Engineering International*, *18*(2), pp.156-165.
- Cornell, C. A. *et al.* (2002). Probabilistic basis for 2000 SAC federal emergency management agency steel moment frame guidelines. *Journal of structural engineering*. American Society of Civil Engineers, 128(4), pp. 526–533.
- Ganey, R.S. (2015). Seismic design and testing of rocking cross laminated timber walls (Doctoral dissertation).
- Guo, H., Liu, Y., Meng, Y., Huang, H., Sun, C. and Shao, Y. (2017). A comparison of the energy saving and carbon reduction performance between reinforced concrete and cross-laminated timber structures in residential buildings in the severe cold region of China. *Sustainability*, 9(8), p.1426.
- Hyo Seon Park, Jin Woo Hwang, Byung Kwan Oh,. (2018). Integrated analysis model for assessing CO2 emissions, seismic performance, and costs of buildings through performance-based optimal seismic design with sustainability. *Energy and Buildings*, *158*, pp.761-775.
- Iman, R.L., Helton, J.C. and Campbell, J.E. (1981). An approach to sensitivity analysis of computer models: Part I—Introduction, input variable selection and preliminary variable assessment. *Journal of quality technology*, *13*(3), pp.174-183.
- Kontra, S., Barbosa, A. R., Sinha, A., Araujo R., G. A., Uarac, P., Brown, N. C., Furley, J., Ho, T. X., Orozco, G. F., Simpson, B. G., van de Lindt, J. W., Zargar, S. H. (2023). Design and Cradle-to-Grave Life-Cycle Assessment: Full-Scale Six-Story Shake-Table Test Building Lateral Systems. *Proceedings of the World Conference on Timber Engineering*. Oslo, Norway.
- Lagaros, N.D., Garavelas, A.T. and Papadrakakis, M. (2008). Innovative seismic design optimization with reliability constraints. *Computer methods in applied mechanics and engineering*, 198(1), pp.28-41.
- Lashof, D.A. and Ahuja, D.R. (1990). Relative contributions of greenhouse gas emissions to global warming. *Nature*, *344*(6266), pp.529-531.
- Liu, Y., Guo, H., Sun, C. and Chang, W.S. (2016). Assessing cross laminated timber (CLT) as an alternative material for mid-rise residential buildings in cold regions in China—A life-cycle assessment approach. *Sustainability*, *8*(10), p.1047.
- Lukacs, I., Björnfot, A. and Tomasi, R. (2019). Strength and stiffness of cross-laminated timber (CLT) shear walls: State-of-the-art of analytical approaches. *Engineering Structures*, *178*, pp.136-147.
- Manfredi, V. and Masi, A. (2018). Seismic strengthening and energy efficiency: Towards an integrated approach for the rehabilitation of existing RC buildings. *Buildings*, *178*, pp.136-147.
- Massari, M., Savoia, M. and Barbosa, A.R. (2017). Experimental and numerical study of two-story post-tensioned seismic resisting CLT wall with external hysteretic energy dissipaters. pp.72-82.
- Menna, C., Vitiello, U., Mauro, G.M., Asprone, D., Bianco, N. and Prota, A. (2019). Integration of seismic risk into energy retrofit optimization procedures: A possible approach based on life cycle evaluation. *In IOP Conference Series: Earth and Environmental Science*. (Vol. 290, No. 1, p. 012022).
- Newcombe, M.P., Pampanin, S., Buchanan, A., Palermo, A. (2008). Section analysis and cyclic behavior of post-tensioned jointed ductile connections. *J Earthquake Eng, 12*(S1), pp.83-110.

Pampanin, S., Priestley, MJN, Sritharan, S. (2001). Analytical modeling of the seismic behavior of precast concrete frames designed with ductile. *J Earthquake Eng*, *5*(03), pp.329-367.

- Park, H.S., Hwang, J.W. and Oh, B.K. (2018). Integrated analysis model for assessing CO2 emissions, seismic performance, and costs of buildings through performance-based optimal seismic design with sustainability. *Energy and Buildings*, *158*, pp.761-775.
- Piacenza, J.R., Tumer, I.Y., Seyedmahmoudi, S.H., Haapala, K.R. and Hoyle, C. (2013). Comparison of sustainability performance for cross laminated timber and concrete. *International Design Engineering Technical Conferences and Computers and Information in Engineering Conference*.
- Sandoli, A., D'Ambra, C., Ceraldi, C., Calderoni, B. and Prota, A. (2021). Sustainable cross-laminated timber structures in a seismic area: Overview and future trends. *Applied Sciences*, *11*(5), p.2078.
- Shargh, G.B. and Barati, R. (2023). Probabilistic assessment of ground motion rotation impact on seismic performance of structures. *Engineering Structures*, *292*, p.116383.
- SmartLam. (2020). Cross-Laminated Timber Specification Guide. (SmartLam).
- van de Lindt, J.W., Furley, J., Amini, M.O., Pei, S., Tamagnone, G., Barbosa, A.R., Rammer, D., Line, P., Fragiacomo, M. and Popovski, M. (2019). Experimental seismic behavior of a two-story CLT platform building. *Engineering Structures* pp.408-422.
- Waldman, B., Hyatt, A., Carlisle, S., Palmeri, J. and Simonen, K. (2023). Carbon Leadership Forum North American Material Baselines-Report & Appendices.
- Wichman, S., Berman, J.W. and Pei, S. (2022). Experimental investigation and numerical modeling of rocking cross laminated timber walls on a flexible foundation. *Earthquake Engineering & Structural Dynamics*, *51*(7), pp.1697-1717.
- Younis, A. and Dodoo, A. (2022). Cross-laminated timber for building construction: A life-cycle-assessment overview. *Journal of Building Engineering*, *52*, p.104482.
- Zakian, P. and Kaveh, A. (2023). Multi-objective Seismic Design Optimization of Structures: A Review. *Archives of Computational Methods in Engineering*, pp.1-16.
- Zargar, H., Uarac, P., Barbosa, A., Sinha, A., Simpson, van de Lindt, J. F., Brown, N. (2023). Comparing optimization approaches in OpenSees-based direct displacement design of tall timber lateral systems. *ASCE International Conferenceon Computing in Civil Engineering*. Corvallis, OR.
- Zhu, M., McKenna, F. and Scott, M.H. (2018). OpenSeesPy: Python library for the OpenSees finite element framework. *SoftwareX*, 7, pp.6-11.